Drosophila Neuronal Glucose 6 Phosphatase is a modulator of Neuropeptide Release that regulates muscle glycogen stores via FMRFamide signaling

Tetsuya Miyamoto, Sheida Hedjazi, Chika Miyamoto and Hubert Amrein

Department of Cell Biology and Genetics

School of Medicine

Texas A&M University

Bryan, Texas

SUMMARY

Neuropeptides (NPs) and their cognate receptors are critical molecular effectors of diverse physiological processes and behaviors. We recently reported of a non-canonical function of the *Drosophila Glucose-6-Phosphatase* (*G6P*) gene in a subset of neurosecretory cells in the CNS that governs systemic glucose homeostasis in food deprived flies. Here, we show that *G6P* expressing neurons define 7 groups of neuropeptide secreting cells, 5 in the brain and 2 in the thoracic ganglia. Using the glucose homeostasis phenotype as a screening tool, we show that one such group, located in the thoracic ganglia and expressing FMRFamide ($FMRFa^{G6P}$) neuropeptides, is necessary and sufficient to maintain systemic glucose homeostasis in starved flies. We further show that the receptor for FMRFamides (FMRFaR) is one key target of *G6P* dependent NP signaling and essential for the build-up of glycogen stores in the jump muscle. Lastly, measurements of the Golgi apparatus of $FMRFa^{G6P}$ neurons and neuropeptide released into the hemolymph suggests that *G6P* enhances FMRFa signaling by increasing the capacity of the neurosecretory system. We propose a general model in which the main role of *G6P* is to counteract glycolysis in peptidergic neurons for the purpose of optimizing the intracellular environment best suited for the expansion of the Golgi apparatus, boosting release of neuropeptides, which through the activation of specific neuropeptide receptors, enhances signaling in respective target tissues.

INTRODUCTION

Neuropeptides (NPs) play central roles in modulating physiology and behaviors. In humans, more than one hundred NPs have been identified, and most of them act through known G protein coupled receptors expressed in specific neurons of the brain or target cells in non-neuronal organs and tissues (Chini, 2019; Hoyer and Bartfai, 2012; Nässel and Zandawala, 2019). *Drosophila melanogaster* has become an important model system for investigating the complex functions of NPs and their receptors, due to the expansive range of molecular genetic tools, the ability to visualize electrophysiological activity and the availability of powerful behavioral assays. More than 40 neuropeptide genes have been described in the fruit fly, many of which encode multiple NPs, and for many of these, putative receptors have been identified (Nässel and Zandawala, 2019). We recently reported expression of the gluconeogenic enzyme Glucose-6-phosphatase (G6P) in small different subpopulations of peptidergic neurons in the fly CNS. By expressing a CFP/YFP based glucose sensor, we showed that *G6P* is functional in these cells by not only maintaining intracellular glucose levels when flies are food deprived, but also as a gluconeogenic enzyme during the conversion of alanine via glucose-6-phosphate (g-6-p) to glucose (Miyamoto and Amrein, 2019). At the systemic level, we found that starved *G6P* mutant flies failed to maintain whole body glucose homeostasis, a phenotype that was not only rescued by expression of a *G6P* transgene, but also by activation of *G6P* neurons using the thermoactive channel TRPA1 (Parisky et al., 2008).

In mammals, G6P is mainly known as a key liver and kidney enzyme during gluconeogenesis and glycogenolysis, metabolic processes upregulated in food-deprived animals. G6P hydrolyses g-6-p to glucose, which is then released into the blood stream to maintain glucose homeostasis. In insects, which share these metabolic pathways, these processes take place in the adipose tissue (fat body) and Malpighian tubules (the “insect’s liver and kidney”) up to the last step. In that last step, g-6-p is converted to trehalose, the main circulating insect sugar, using the enzyme trehalose 6 phosphate synthase 1 (TPS1) to ensure sugar homeostasis when flies are starved (Matsuda et al., 2015; Thompson, 2003). Thus, the existence of a conserved *Drosophila* G6P enzyme in general, and the expression of G6P in peptidergic neurons specifically, which are not known to be involved in systemic sugar homeostasis, raises intriguing questions about its function in NP signaling. First and foremost, what is the neuronal identity of the approximately 30 *G6P-GAL4* expressing neurons in the CNS, beyond the fact that these neurons express DIMM, a marker for large NP producing

neurons (Hewes et al., 2003)? Second, which of these neurons mediate whole body glucose homeostasis in starved flies, the currently only know function of *G6P*? Third, what is the cellular role of G6P in peptidergic neurons? And fourth, what is the primary phenotype that ultimately leads to failed glucose homeostasis in starved *G6P* mutant flies?

In this paper, we have provided answers to these questions. We determined the identity of *G6P* neurons in the fly CNS by correlating *G6P-GAL4* expression with the location of NP producing neurons. Specifically, we identified subsets of large neuropeptide F (NPF), Orcokinin A (OrcoA), pigment-dispersing factor (Pdf), FMRFamide and IPNamide - positive neurons that also express *G6P-GAL4.* By inhibiting neural activity and rescuing G6P function in $G6P^{-/-}$ flies in each of these subsets, we show that *FMRFa* expressing *G6P* ($FMRFa^{G6P}$) neurons located in the thoracic ganglia ($FMRFa^{GP6}$) alone are necessary and sufficient to maintain whole body glucose homeostasis in food deprived flies. Moreover, we find that the gene encoding the receptor for FMRFamides (*FMRFaR*) is predominantly expressed in the jump muscle, where it plays a critical role in establishing glycogen stores. Specifically, glycogen content in the jump muscle of fed $G6P^{-/-}$, $FMRFa^{-/-}$ and $FMRFaR^{-/-}$ flies is reduced by about 50% compared to fed wild type controls, indicating that FMRFa-FMRFaR signaling is essential to build up glycogen stores. Lastly, we describe the first cellular phenotypes associated with *G6P* in *FMRFa* neurons, a smaller Golgi apparatus and reduced NP release from $FMRFa^{G6P}$ neurons. We propose that G6P counteracts glycolysis in NP secreting neurons, thereby establishing a cellular environment that is more amenable to the expansion of the Golgi apparatus and large dense core vesicles, which in turn enhances NP release.

RESULTS

Identification of *G6P-GAL4* neuronal subtypes

Initial expression analysis of *G6P-GAL4; UAS-GFP* flies revealed the presence of approximately 14 GFP positive neurons in the brain (Miyamoto and Amrein, 2019). Three lines of evidence suggested that most, if not all, *G6P* expressing neurons were NP producing cells: First, they are relatively large in appearance and express DIMM, a transcriptional regulator that plays a key role in cell fate determination of NP producing cells (Hewes et al., 2003). Second, one pair of cells located in the dorsomedial region co-expresses NPF, a *Drosophila* homolog of mammalian NPY. And third, examination of *G6P* expression in the thoracic

ganglion showed many additional *G6P* positive cells, in a pattern similar to that of FMRFamide and IPNamide neuropeptides (Lundquist and Nässel, 1990; Schneider et al., 1993b; Verleyen et al., 2004). These observations suggested that *G6P* is found in diverse populations of peptidergic neurons, expressing different NPs. We therefore set out to determine the identity of these NPs by comparing locations of G6P positive neurons with available reports of NP expression profiles, comprehensively reviewed by Nässel and Zandawala (Nässel and Zandawala, 2019). Based on this comparison, we carried out double staining experiments of brain and thoracic ganglia preparations of *G6P-GAL4*; *UAS-mCD8GFP* flies using NP specific antibodies and identified five NPs co-expressed with small subsets of *G6P* neurons (Figure 1). In the brain, in addition to the prominent pair of $G6P^{NPF}$ neurons, Orcokinin-A-, PDF- and IPNa-positive neurons were found to be expressed in subsets of *G6P-GAL4* neurons (Figure 1A-1E, referred to as $Oroco^{G6P}$, PDF^{G6P}, $IPNa^{Br_G6P}$ neurons), while in the thoracic ganglion, a group of FMRFa-positive neurons and a second subset of IPNa-positive neurons were present (Figure 1G-1I, referred to $FMRFa^{G6P}$ and $IPNa^{Th_G6P}$ neurons; note that the FMRFa-positive neurons present in the brain do not express *G6P-GAL4*). Neurons expressing a given NP fall generally into two groups: a small number of neurons with large cell bodies, and a larger number with relatively small body size (Figure 1). For example, in the brain, there are some 20 NPF expressing neurons, only four of which fall into the large size class (Shao et al., 2017) (Figure 1J). Likewise, only two of the 10 Orcokinin positive neurons fall into the large class. Of note, G6P is only expressed in the large type of cells, both in the brain and the thoracic ganglion (Figure 1B-1E, 1H and 1I). Together, about 30 of the 60 large neurons expressing the five NPs are G6P-positive, while all small neurons are G6P-negative (Figure 1J).

In order to functionally manipulate subpopulations of specific NP expressing neurons, we procured *GAL4* lines expressed in Orcokinin, IPNa and FMRFa producing neurons from the *Flylight* repository (https://www.janelia.org/project-team/flylight) or obtained previously characterized lines for NPF (Wu et al., 2003) and PDF (Renn et al., 1999), respectively. We confirmed *GAL4* expression with these NPs by co-immunostaining brains and thoracic ganglia of *NP-GAL4; UAS-mCD8GFP* flies (Supplementary Figure 1).

FMRFa peptides mediate glucose homeostasis

Expression of *G6P* in different NP secreting neurons suggests that G6P activity impacts several distinct NP signaling pathways. Using *G6P* mutant flies, we previously showed that

one function of this enzyme is to maintain whole-body glucose homeostasis in starved flies, while having no significant impact on the levels of trehalose. Importantly, whole-body glucose homeostasis can be complemented in *G6P* mutant flies by temperature induced neural activation of *G6P* neurons (Miyamoto and Amrein, 2019) using *UAS-TRPA1* (Parisky et al., 2008). Similarly, silencing all *G6P-GAL4* expressing neurons using *UAS-Kir2.1* encoding the inward rectifier potassium channel Kir2.1 (Baines et al., 2001; Paradis et al., 2001) mimicked whole-body glucose homeostasis phenotype of *G6P* mutant flies (Figure 2A)(Miyamoto and Amrein, 2019). To determine which of the five NP expressing cell types is responsible for glucose homeostasis, we expressed *UAS-Kir2.1* under the control of the five NP specific *GAL4* drivers. Inactivation of NPF^{G6P}, $Orco^{G6P}$, PDF^{G6P}, or $IPNa^{TG_G6P}$ neurons caused no change in whole body glucose levels in either feeding condition (Figure 2A). Only expression of *UAS-Kir2.1* in $FMRFa^{G6P}$ neurons (*GMR18C05-GAL4*) led to significantly reduced glucose levels in starved flies (Figure 2A). Consistent with our previous analysis, trehalose levels were not significantly different in any of these flies when compared to wild type control flies (Supplementary Figure 3). To test whether the function of *G6P* in *FMRFa* positive neurons is sufficient for maintaining whole body glucose homeostasis, we measured glucose levels in *G6P* mutant flies expressing a *UAS-G6P* transgene under the control of *GMR18C05-GAL4*. Indeed, these flies showed fully restored whole body glucose levels under starving conditions (Figure 2B). Taken together, these experiments identified $FMRFa^{G6P}$ neurons in the thoracic ganglion as the neurons responsible for maintaining whole body glucose homeostasis in food deprived flies.

The *FMRFa* gene encodes a 347 amino acid long propeptide, which is processed into 16 peptides, 10 of which are 7 to 9 aa long and characterized by the caroboxyterminal FMRF motif (Figure 2C). To further confirm that FMRFamides are the signaling molecules mediating glucose homeostasis in starved flies, we measured glucose levels in $FMRFa^{P}$ mutant flies. $FMRFa^{P}$ is a P-element insertion into the 10th of the 16 peptides and homozygous $FMRFa^{P}$ mutant, starved flies showed the same glucose homeostasis deficit as flies in which these neurons were silenced (Figure 2D). We also used a CRISPR/CAS-9 gene knock-out strategy to generate additional *FMRFa* mutations. This resulted in several additional alleles, one of which was a deletion encompassing all 16 peptides (*ΔFMRFa*, Figure 2C, Supplementary Figure 2) that caused reduced whole body glucose levels in both fed and starved flies (Figure 2D).

G6P is necessary to maintain glucose levels in *FMRFa^{G6P}* neurons

NPF^{G6P} neurons in the brain require G6P cell-autonomously to maintain intracellular glucose levels when flies are starved which we established in whole brain preparations, as well as live glucose imaging experiments using the fluorescent sensitive glucose sensor Glu700 (Miyamoto and Amrein, 2019). While the relevance for this phenomenon for proper neuropeptide signaling remains to be determined, the glucose sensor provides a means to assess whether G6P is functionally relevant for maintaining intracellular glucose levels during starvation. Thus, we established an *in vivo* preparation of the ventral nerve cord that allowed as to monitor glucose levels in *FMRFa^{G6P}* neurons of the thoracic ganglion (see Material and Methods). Since G6P is an Endoplasmic Reticulum (ER) resident enzyme (van Schaftingen and Gerin, 2002), we expressed an ER resident version *Glu700, Glu700KDEL* (Addgene, #17867) under the control of *GMR18C05-GAL4*. In fed *G6P* mutant flies, glucose levels were indistinguishable from wild type fed flies, while in starved flies, *G6P* mutants showed significantly lower glucose levels compared to fed flies (Figure 3). Importantly, whole body glucose homeostasis of starved *G6P* mutants was fully restored when a *UAS-G6P* transgene was expressed in these neurons. Together, these results show that in starved flies, G6P is also functional in *FMRFa^{G6P}* neurons where it maintains intracellular glucose levels during starvation.

G6P increases Golgi network volume and facilitates NP release

NP processing involves propeptide cleavage and transition of NPs through the Golgi network, ultimately leading to NP deposition in Large Dense Core Vesicles (LDCVs) that derive from the trans Golgi stack (van den Pol, 2012). Thus, we examined whether any difference in size and overall distribution of the ER and Golgi network of *FMRFa^{G6P}* neurons were apparent between *wild type* and *G6P* mutant flies using ER (GFP-KDEL)(Kneen et al., 1998) and Golgi (αManll-GFP) resident reporter proteins (Hardt et al., 2005; Zhou et al., 2014). No obvious differences were observed in the ER. However, the Golgi network occupied a significantly smaller area in *G6P* mutant flies compared to *wild type* flies (Figure 4A 9% vs 14%). A similar reduction in Golgi volume was also observed when these reporters were express in the pair of *NPF^{G6P}*neurons (9% vs 16%, Figure 4B; left panels). Of note, and in contrast to mammalian

cells where the Golgi complex is organized as a single ribbon, the *Drosophila* Golgi apparatus is dispersed throughout the cytoplasm (Kondylis and Rabouille, 2009).

Because LDCVs emerge from the trans Golgi network, one may expect that NP release to be reduced in *G6P* mutant flies when compared to *wild type* flies. To measure the effect of G6P on NP release, we took advantage of the fact that the *FMFRa*^{G6P} neurons represent a subset of Tv neurons, which innervate the neurohemal organ, a tissue specialized for neurosecretion into the hemolymph (Lundquist and Nässel, 1990; Schneider et al., 1993b). Thus, FMRFa release from *FMFRa*^{G6P} neurons can be assessed by measuring the FMRFa amounts in the hemolymph. Because available antibodies against FMRFa cross-react with hemolymph components/peptides (data now shown), we used the mammalian Atrial natriuretic peptide (Anf) fused to GFP as a proxy NP (Anf-GFP, Husain and Ewer, 2004) by assessing Anf-GFP hemolymph concentration in *wild-type* and *G6P* mutant flies (Figure 5). Anf-GFP is released in a time-appropriate fashion during molting, following the dynamic profile of the resident peptides in these cell, Ecdysis Triggering Hormone (Husain and Ewer, 2004). We expressed the *UAS-Anf-GFP* reporter gene in *FMFRa*^{G6P} neurons and measured peptide levels in the hemolymph. Compared to the *wild-type*, *G6P* mutant flies secrete significantly lower amounts of Anf-GFP into the hemolymph (Figure 5A). This phenotype is observed in both feeding states, but the difference is more pronounced in starved flies. Importantly, the deficit can be rescued by inclusion of a *UAS-G6P* transgene. To explore whether G6P dependence can be imposed on non-*G6P* neurosecretory cells, we measured hemolymph levels of an epitope tagged, Insulin like peptide 2 (Ilp2), expressed from a genetically modified *Ilp2* gene (*Ilp2*^{1} *gd2HF*) (Park et al., 2014). When *UAS-G6P* was expressed in insulin producing cells (IPCs; *Ilp2*^{1} *gd2HF/dilp2-GAL4 UAS-G6P*), a significant increase of Ilp2HF was observed in the hemolymph, when compared to control flies lacking the *UAS-G6P* transgene (Figure 5B). Two observations are noteworthy: first, Ilp2HF secretion levels are similar in fed and starved flies. This is not unexpected, as Ilp2HF increase is highly transient and observed in only starved and re-fed flies up to 90 minutes after refeeding (Park et al., 2014). In our paradigm, fed flies are not previously starved, and hence no transient Ilp2HF increase is expected. Second, and unlike Anf-GFP secretion from *FMRFa*^{G6P} neurons, exogenous G6P expression increased hemolymph Ilp2HF levels only in starved flies. This might be due to the fact that endogenous Ilp2 secretion is minimal during food deprivation, and expression of G6P noticeably elevates secretion from this low base level. In fed flies, the

secretion machinery is already maximally primed and G6P expression might not increase secretion any further. In conclusion, G6P presence in peptidergic neurons enhances their capabilities to secrete NPs.

G6P mediated FMRFa signaling to the jump muscle for glycogen storage

In invertebrates, FMRFamides have been associated with the regulation of heart rate gut motility, as well as propagation (Nässel and Zandawala, 2019). Yet, the function of FMRFamides and their receptors has remained largely elusive, in part because these studies have been conducted in systems not amenable to molecular genetic analyses. Thus, we sought to determine the tissue in which the FMRFa receptors (FMRFaR, CG2114) is expressed and identify phenotype(s) in the respective target tissue of flies carrying *FMRFaR* mutations. We took advantage of the chemoconnectomics resource reported by Deng and colleagues, who generated a series of *GAL4* knock-in lines for many NP receptor genes, including *FMRFaR* (Deng et al., 2019). In adult flies, $FMRFaR^{2A\text{-}GAL4}$ is strongly expressed in the jump muscle, with moderate expression in the CNS, while no expression was found in other tissues (flight muscle, reproductive system, fat body, gut etc; Figure 6A), a finding consistent with expression profiles reported in the aging fly cell atlas (Lu et al., 2023). We acquired a *FMRFaR* mutant strain ($FMRFaR^{MB04659}$) and examined the amount of muscle glucose and glycogen in *wild type* and homozygous receptor mutant flies (Figure 6B). While free glucose levels were not noticeably different in the jump muscle, regardless of feeding status, muscle glycogen was significantly lower in fed $FMRFaR^{MB04659}$ homozygous mutant flies (Figure 6B). This loss was fully rescued in the presence of a *UAS-FMRFaR* transgene driven by *Act79B-GAL4* (Figure 6C), which is predominantly expressed in the jump muscle (Bryantsev et al., 2012). Of note, the presence of *ELAV-GAL80* in these flies eliminates any potential FMRFaR contribution from low expression of *Act79B-GAL4* in the CNS. Furthermore, glycogen levels were also significantly reduced in fed *G6P* and *FMRFa* mutant flies, to similar levels found in *FMRFaR* mutants (Figure 6D). Taken together, these results indicate that one key function of FMRFa signaling is the generation of glycogen stores that can be accessed in times of limited nutrient availability.

DISCUSSION

Activity of NPs is dependent on many external and internal factors, providing a means for temporally and quantitatively controlled release that accommodates animals'

physiological demands. In addition to transcriptional and RNA processing regulation (Gauthier and Hewes, 2006; Herzog et al., 1997; Higuchi et al., 2005; Schneider et al., 1993a), most NPs undergo post-translational modification through proteolytic cleavage from precursor proteins (pro-peptides) (van den Pol, 2012). Generally, these processes are at least to some extent unique for each NP, since they are linked to specific features of the NP gene promoter or its gene products (mRNA, pro-peptide). The studies presented here report a new mode of regulation in NP signaling, which allows modulation across distinct types of secretory neurons expressing the gluconeogenic enzyme G6P. Based on measurement of hemolymph Anf-GFP peptide expressed in *FMRFa*^{G6P}neurons and Ilp2HF produced in IPCs ectopically expressing a *UAS-G6P* transgene, we postulate that G6P primes peptidergic neurons for more efficient NP release, regardless of the NP they express. Given its expression profile, G6P likely modulates a range of physiological processes and behaviors, including courtship (NPF; Liu et al., 2019; Silva et al., 2021), oogenesis (Orcokinin, Silva et al., 2021), circadian behavior and sleep (PDF, Chung et al., 2017; Lear et al., 2009; Parisky et al., 2008), as well as feeding (NPF, Landayan et al., 2021; Lear et al., 2009; Lee et al., 2004). To our knowledge, a role for an enzyme with an established role in gluconeogenesis and glycogenolysis in neurosecretion, or neurons in general, is unprecedented. While a specific mechanism by which G6P modulates peptidergic neurons remains to be determined, the diminished Golgi size in *G6P*^{MIC} neurons implies that G6P activity creates a cellular environment that is beneficial to Golgi expansion (see below).

Cellular mechanisms of G6P on neuropeptide release

The function of mammalian G6P is to catalyze hydrolysis of g-6-p during glycogenolysis or gluconeogenesis, generating free glucose that is exported and released into the blood for systemic glucose homeostasis when animals are food deprived. Despite the fact that *Drosophila* G6P has that same catalytic activity in peptidergic neurons, where it can produce glucose from amino acid precursors (Miyamoto and Amrein, 2019), and *G6P's* requirement to maintain systemic whole-body glucose levels, multiple lines of evidence argue against the notion that peptidergic neurons produce glucose for systemic sugar homeostasis. First and foremost, we have previously shown that glucose homeostasis can be restored in starved *G6P*$^{-/-}$ flies by expression of TRPA1, a thermosensitive transient receptor potential channel, arguing for a signaling role of *G6P* in these neurons (Miyamoto and Amrein, 2019). Second, neurons in general have high energy demands and are ill equipped for the generation of

glucose, for which major amounts of stored glycogen or incidental supply of amino acids is required. Third and related to the point 2, while *G6P* peptidergic neurons are diverse, their primary purpose is to produce and secrete NPs, an energy costly process that seems incompatible with an energy consuming activity such glycogenolysis or gluconeogenesis. And last, in nutrient deprived flies, the fat body is well equipped to maintain sugar homeostasis by generating trehalose from g-6-p. These observations, and the fact that neuronal glycolysis is largely dispensable (see below), lead us to posit that the function of *G6P* is to counteract glycolysis in these peptidergic neurons, creating conditions that are overall beneficial to the main task of these neurons, the release of NPs.

Glycolysis is dispensable in neurons, as was shown by Volkenhoff and colleagues (Volkenhoff et al., 2015). Specifically, pan neuronal RNAi knock down of numerous glycolytic enzymes in the CNS had no impact on survival and overall locomotion, while ubiquitous or pan glial knock-down of the same genes led to lethality or severe locomotion deficits (Volkenhoff et al., 2015). These authors also showed that glial glycolysis is essential for neuronal survival and that the generated lactate is shuttled to neurons, where it is used for ATP production via the TCA cycle. Thus, while (some) neurons might use glycolysis for energy production, it is apparent that they rely metabolites from glia that are feeding other metabolic processes. Based on these findings and our observation that G6P positive peptidergic neurons have higher glucose levels than G6P negative ones (Miyamoto and Amrein, 2019), we posit that inhibition of glycolysis in these neurons creates a cellular environment that enhances production, transport and secretion of NPs. For example, shutdown of glycolysis reduces the amounts of glycolytic metabolites, which will affect the intracellular pH and hence might affect efficacy of numerous biochemical processes, which may be beneficial for the expansion of the Golgi apparatus and ultimately for NP transport and/or secretion.

Diverse roles for G6P enzymes

Humans and most mammals have two additional genes encoding G6P, *G6PC2* expressed in the pancreas, Müller glia cells and spermatids, and the ubiquitously expressed *G6PC3*. *G6PC2* deficient mice show lower fasting blood glucose (Bosma et al., 2020), while humans with mutations in *G6PC3* present with heart defects and neutropenia (Banka et al., 2011; Cheung et al., 2007). An intriguing underlying cellular mechanisms for neutropenia has

been proposed (Veiga-da-Cunha et al., 2019), namely the accumulation of 1,5-anhydroglucitol-6-phosphate (1,5AG6P), a toxic metabolite from a common circulating food compound (1,5-anhydroglucitol), due to lack of G6PC3. This is consistent with the observation that *G6PC3*$^{-/-}$ neutrophils express numerous markers indicative of ER stress, while also exhibiting glycosylation defects (Hayee et al., 2011). Moreover, *G6PC3*$^{-/-}$ neutrophils exhibit reduced glycolysis (Jun et al., 2010). Thus, it appears that the main role of G6PC3 in neutrophils, similar to the function of G6P in *Drosophila* peptideric neurons, is to remove a metabolite that is detrimental to optimal performance of the respective cells. Alternative - and potentially neuronal - roles for G6P enzymes are also indicated by evolutionary arguments, because the *G6P* genes came into existence in Cnidaria, the first animal lineages that possessed neuronal cell types, but lacked organs comparable to the liver or even a basic circulatory system (Miyamoto and Amrein, 2017).

FMRFa-FMRFaR signaling is essential to build up muscle glycogen stores

Our investigations have identified an important primary function for FMRFamides in glycogen metabolism. *Wild type* flies have considerable glycogen stores in muscle, from which they draw upon through glycolysis when deprived of food. In contrast, *G6P*^{MIC}, *ΔFMRFa* and *FMRFaR*^{MB04659} mutant flies have already severely depleted glycogen levels at the outset before they are subjected to food deprivation, and the glycogen these flies can mobilize is limited. For example, muscle glycogen levels during a 24 hour starvation regimen drops by 0.08 µg/µg protein in *wild type* flies, compared to 0.03 µg/µg protein or less in mutants (Figure 6B, supplementary figure 4). Thus, one possibility is that in flies lacking the FMRFaR and unable to boost glycogen reserves, energy needs in the jump muscle are provided through other tissues rich in carbohydrate, such as the adipose, which might explain the whole body glucose deficits in starved *G6P*^{MIC}, *ΔFMRFa* and *FMRFaR*^{MB04659} mutant flies.

A genetically established function for the FMRFaR has been reported in the CNS (Ravi et al., 2018). In this study it was shown that FMRFaR functions in dopaminergic neurons for sustained flight. However, possible metabolic deficits in these flies or the involvement of FMRFamides as signaling molecules was not investigated. Yet, it is intriguing to speculate that energy for sustained flight also requires stored glycogen, possibly provided from other organs. Regardless, muscle has gained considerable attention as a metabolic hub communicating with other organs, including the brain, gut and adipose tissue (Demontis et al., 2013, 2013;

Gomarasca et al., 2020; Rai and Demontis, 2016; Zhao et al., 2020; Zhao and Karpac, 2017). Thus, our work here - and possibly that of Ravi and colleagues - have implicated FMRFa signaling as one likely source in the regulation of systemic nutrient metabolism across different organ systems.

Figure Legends

Figure 1. *G6P* is co-expressed in diverse subsets of peptidergic neurons.

A-F) Antibody staining of the brain (**A-F**) and in the thoracic ganglia (**G-H**) of *G6P-GAL4; UAS-mCD8GFP* flies using anti-GFP antibody and antibodies against the indicated neuropeptides. *G6P-GAL4* is expressed in about 14 neurons in the brain, including a pair of large, centrally located NPF neurons (**B**) and a pair of large Orcokinin-A expressing neurons (**C**), two IPNa (**D**) and four PDF neurons (**E**) which correspond l-LNvs. In the thoracic ganglia, *G6P-GAL4* and is expressed in about 16 neurons, including two pairs of FMRFa neurons (**H**) and four pairs of IPNa neurons (**I**).

I) Expression summary of *G6P-GAL4* neurons and relevant NP is shown in the cartoon. Co-expressing neurons are outlined with a broken line. Note that all *G6P-GAL4* neurons are of the large variety.

Figure 2. G6P mediates whole-body glucose homeostasis through FMRFa neurons.

A) Silencing of all *G6P-GAL4* neurons or *GMR18C05-GAL4* (i.e. *FMRFa* expressing neurons; see Supplementary Figure 1), but not silencing of any other subgroup of neurons, significantly reduces whole body glucose levels. *GMR13H04-GAL4* is expressed in $OrcoA^{G6P}$ neurons, *GMR37G02-GAL4* in $IPNa^{Br_G6P}$ neurons, *GMR39A01-GAL4* in $IPNa^{Th_G6P}$ neurons and *GMR18C05-GAL4* in $FMRFa^{G6P}$ neurons. Asterisks indicate *P<0.05 using Kruskal-Wallis with Dunn's post-hoc test; n=8-10. Error bars represent standard error.

B) *G6P* is required in *FMRFa* neurons for whole body glucose homeostasis in starved flies. Under fed conditions, both *wild-type* and *G6P* mutant flies maintain glucose levels (left). However, when starved for 24 hours, *G6P* mutant flies exhibit significantly reduced whole body glucose levels, a phenotype rescued when a *UAS-G6P* transgene is expressed in $FMRFa^{G6P}$ neurons under the control of *GMR18C05-GAL4*. Asterisks indicate *P<0.05

using Kruskal-Wallis with Dunn's post-hoc test; n=9-12. Error bars represent standard error.

C) Structure of the second, ORF containing exon of the wild type *FMRFa* gene and the *FMRFa[P]* and *ΔFMRFa* mutation. Exon 2 contains all 14 FMRFamides and FMRFamide-related peptides. The P-element in *FMRFa[P]* is inserted in the 11th peptide, while all peptides are deleted in *ΔFMRFa*.

D) FMRFamides are required for whole body glucose homeostasis. Like *G6P* mutants, *FMRFa[P]* mutants have significantly lower glucose levels in starved but not fed conditions. *ΔFMRFa* mutant flies show a lower glucose level regardless of feeding conditions. Asterisks indicate *P<0.05, **P<0.01 using one-way ANOVA with Kruskal-Wallis using Dunn's post-hoc test; n=8-12. Error bars represent standard error.

Figure 3. *G6P* is required to maintain glucose levels in FMRFa neurons of food-deprived flies. Glucose levels were measured using Glu700KDEL, a FRET-based, ER tagged glucose sensor, in FMRFa neurons in the thoracic ganglion of *GMR18C05-GAL4/UAS-Glu700KDEL* flies. Glucose levels are reduced in starved *G6P* mutant flies, which was rescued in the presence of a *UAS-G6P* transgene. Asterisk indicates **P<0.01 using one-way ANOVA with Tukey post hoc test. N=8-17. Error bars represent standard error.

Figure 4. G6P positively affects the size of Golgi apparatus in the peptidergic neurons.
The Golgi apparatus was visualized by expressing the GFP tagged Golgi marker UAS-ManII-eGFP. FMRFa staining was used as a proxy for cell body. Golgi size was normalized by cell body size. $FMRFa^{G6P}$ (A) and NPF^{G6P} (B) neurons of $G6P^{-/-}$ flies have a significantly smaller Golgi apparatus, both in fed and starved flies. This phenotype is rescued by expressing *UAS-G6P* transgene. Asterisks indicate *P<0.05 using Kruskal-Wallis with Dunn's post-hoc test. N=44-65 for $FMRFa^{G6P}$ neurons, N=12-23 for NPF^{G6P} neurons. Error bars represent standard error. Scale bars are 4µm.

Figure 5: FMRFa neurons require G6P for efficient neuropeptide secretion.

A) Neuropeptide secretion was quantified using *UAS-Anf-GFP*, a neuropeptide reporter expressed in *FMRFa* neurons using the *GMR18C05-GAL4* driver. Anf-GFP was measured in the hemolymph using a Rat ANP ELISA Kit (abcam, ab108797). Compared

to *wild-type*, the hemolymph of *G6P* mutant flies shows significantly lower Anf-GFP levels in both the fed and starved flies. Secretion of Anf-G6P is rescued in the presence of a *UAS-G6P* transgene.

B) Secretion from IPCs was quantified using the *Ilp2*^{1} *gd2HF* strain, which carries a genetically tagged Ilp2 allele. Ectopic expression of *UAS-G6P* under the control of *dilp2-GAL4* increased Ilp2HF levels in the hemolymph of starved flies. Asterisks indicate **P<0.01 using Kruskal-Wallis with Dunn's post-hoc test. N=12 for *FMRFa*^{G6P} neurons. N=9 for IPC. Bars represent standard error.

Figure 6: FMRFa acts on the FMRFa receptor to establish glycogen stores in the jump muscle

A) *FMRFaR* was visualized using the *GAL4* gene knock in (*FMRFaR*$^{2A\text{-}GAL4}$) combined with a *UAS-mCD8GFP* reporter, following anti-GFP staining, showing robust and modertate expression in the jump muscle and CNS, respectively. Preparation was counterstained by Phalloidin (Invitrogen A34055).

B) Glycogen stores in the jump muscle were significantly reduced in the *FMRFaR*^{MB} mutant flies in fed and starved conditions, while glucose levels remained unchanged.

C) Glycogen stores were restored to *wild type* levels when *UAS-FMRFaR* was in the jump muscle in *FMRFaR*^{MB} mutant flies also containing *ELAV-GAL80* suppressor.

D) Glycogen deficiencies in the jump muscle are consistently observed in the *G6P*^{MIC} and *ΔFMRFa* mutant flies.

Asterisks indicate *P<0.05, **P<0.01 by one-way ANOVA using Kruskal-Wallis with Dunn's post-hoc test. n=7-14. Error bars represent standard error.

Supplementary Figure 1: Identification and Expression of Gal4 lines labeling specific peptidergic neurons

A-B) Brains of flies expressing *UAS-mCD8GFP* driven by *NPF-GAL4* (Wu et al., 2003) and *PDF-GAL4* (Renn et al., 1999) were double-stained with antibodies against GFP and NPF (**A**) and PDF (**B**) respectively, revealing co-expression in all GAL4 expressing neurons.

C-F) Neuropeptide specific *FlyLight GAL4* lines *GMR13H04*, *GMR37G02*, *GMR39A01* and *GMR18C05* were identified by comparing expression profiles with antibody staining data (Nässel and Zandawala, 2019, and references therein). We double stained the CNS of these lines in the presence of a *UAS- mCD8GFP* reporter with anti-GFP and neuropeptide specific

antibodies, which revealed almost total co-expression of neurons expressing Orcokinin A (**C**), IPNa (**D** and **E**) and FMRFamides (**F**).

Supplementary Figure 2. Thoracic ganglia expression of FMRFamides in the *wild-type*, *FMRFa[P]* and *ΔFMRFa* mutant flies. Immunostaining was performed using anti-FMRFa antibody. Note the absence of any immunoreactivity in *ΔFMRFa* mutant flies.

Supplementary Figure 3. Whole body trehalose does generally not significantly differ when subsets of *G6P* neurons are inactivated by expression of Kir2.1. We note that the level of trehalose is increased when *NPF* neurons are inactivated. Asterisks indicate *P<0.05 by Kruskal-Wallis with Dunn's post-hoc test; n=8-10. Error bars represent standard error.

Supplementary Figure 4. Glycogen stores in the jump muscle of *wild type* and $G6P^{MIC}$, *ΔFMRFa* and $FMRFaR^{MB}$ mutant flies. The reduced glycogen stores in the jump muscle of fed mutant flies are further reduced, but the Asterisks indicate *P<0.05, **P<0.01 by Mann-Whitney U-test. n=7-14. Error bars represent standard error.

ACKNOWLEGEMENTS

We thank Dr. Paul Hardin for *Pdf-GAL4* flies, Dr. Gaiti Hasan for *UAS-FMRFaR* flies, Dr. Wolf Frommer for the Glu700KDEL plasmid (Addgene plasmid #17867) and Dr. Simon Bullock for pCFD3 plasmid (Addgene plasmid #49410). Antibody gifts were provided by Dr. Mizoguchi (anti-Orcokinin), Dr. Thor (anti-IPNa) and Dr. Hardin (anti-PDF). We thank Drs. Dick Nässel and Raquel Sitcheran for valuable comments on the manuscript. We are grateful to Anastasia Lucas and Edward Wang for assistance on the metabolic assays. This work was supported by an NIH grant 1R21NS118118-01 awarded to H.A.

MATERIAL AND METHODS

Fly strains and maintenance

Experiments were performed using adult *Drosophila melanogaster* males, aged between 7-14 days. Flies were reared on the standard fly food containing cornmeal, yeast and sugar at

23-24˚C. *G6P*^{MI12250} is referred as *G6P*^{MIC}, *FMRFa*^{KG01300} is referred as *FMRFa*^{P}, *FMRFaR*^{MB04659} is referred as *FMRFaR*^{MB}. The exact phenotypes used in each experiment were as follows (from left to right):

Figure 1: *w; G6P-GAL4; UAS-mCD8GFP*.

Figure 2: (A) *yw; UAS-Kir2.1*, *yw; G6P-GAL4/UAS-Kir2.1*, *yw; NPF-GAL4/UAS-Kir2.1*, *yw; UAS-Kir2.1; GMR13H04-GAL4*, *yw; UAS-Kir2.1; GMR37G02-GAL4*, *yw; UAS-Kir2.1; Pdf-GAL4*, *yw; UAS-Kir2.1; GMR18C05-GAL4*, *yw; UAS-Kir2.1; GMR39A01-GAL4*. (B) from left to right, *yw*, *yw; G6P*^{MIC}*/G6P*^{MIC}, *yw; G6P*^{MIC}*/G6P*^{MIC}*; GMR18C05-GAL4*, *yw; G6P*^{MIC}*/G6P*^{MIC}*; UAS-G6P*, *yw; G6P*^{MIC}*/G6P*^{MIC}*; GMR18C05-GAL4/UAS-G6P*. (D) from left to right, *yw*, *yw; G6P*^{MIC}*/G6P*^{MIC}, *yw; FMRFa*^{P}*/FMRFa*^{P}, *yw; ΔFMRFa/ΔFMRFa*.

Figure 3: *w; UAS-Glu700KDEL; GMR18C05-GAL4*, w;*G6P*^{MIC} *UAS-Glu700KDEL/G6P*^{MIC}*; GMR18C05-GAL4*, *w; G6P*^{MIC} *UAS-Glu700KDEL/G6P*^{MIC}*; GMR18C05-GAL4/UAS-G6P*.

Figure 4: (A) *w; UAS-ManII-eGFP; GMR18C05-GAL4*, w; *G6P*^{MIC} *UAS-ManII-eGFP/G6P*^{MIC}*; GMR18C05-GAL4*, *w; G6P*^{MIC} *UAS-ManII-eGFP/G6P*^{MIC}*; GMR18C05-GAL4/UAS-G6P*.

Figure 5: (A) *UAS-AnfGFP; GMR18C05-GAL4*, *UAS-AnfGFP; G6P*^{MIC}*/G6P*^{MIC}*; GMR18C05-GAL4, UAS-AnfGFP; G6P*^{MIC}*/G6P*^{MIC}*; GMR18C05-GAL4/UAS-G6P.* (B) from left to right, *w; Ilp2*^{1} *gd2HF/dilp2-GAL4, w; Ilp2*^{1} *gd2HF/UAS-G6P, w; Ilp2*^{1} *gd2HF/dilp2-GAL4 UAS-G6P.*

Figure 6 (A) *w;FMRFaR*$^{2A-GAL4}$*/UAS-mCD8GFP*. (B) *yw*, *yw; FMRFaR*^{MB}. (C) *yw*, *yw; FMRFaR*^{MB}, *Act79B-GAL4; ELAV-GAL80; FMRFaR*^{MB}*, yw; FMRFaR*^{MB} *UAS-FMRFaR/FMRFaR*^{MB}*, Act79B-GAL4 ; ELAV-GAL80; FMRFaR*^{MB} *UAS-FMRFaR/FMRFaR*^{MB}*.* (D) *yw*, *yw; G6P*^{MIC}, *yw; ΔFMRFa*.

NPF-GAL4 (#25681), *GMR13H04-GAL4* (#48589), *GMR37G02-GAL4* (#49965), *GMR18C05-GAL4* (#47330), *GMR39A01-GAL4* (#45667), *UAS-Kir2.1* (#6596), *G6P*^{MIC} (#57904), *FMRFa*^{KG01300} (#13717), UAS-ANF-GFP (#7001) flies were obtained from Bloomington Stock Center. *Pdf-GAL4* flies were obtained from Dr. Paul Hardin. Glu700KDEL was a gift from Dr. Wolf Frommer (Addgene plasmid #17867). *UAS-FMRFaR* flies were obtained from Dr. Gaiti Hasan. *Ilp2*^{1} *gd2HF* flies were obtained from Dr. Seung Kim. *G6P-GAL4*, *UAS-G6P* and *ΔFMRFa* were generated in Amrein lab.

Quantification and Statistical Analysis

Statistical significance was calculated using Student's t-test or two-tailed Mann-Whitney U test for pairwise comparisons, and one-way ANOVA with Tukey post hoc test or Kruskal-

Wallis test with Dunn's post-hoc test for multiple comparisons. Error bars are standard error of the mean (SEM) except where noted. Significance: *p<0.05, **p<0.01, NS: not significant. All replicates are from different biological samples (testing different flies or cells). Image analysis was performed with NIS-Elements software suite. Statistical analysis was performed in Real Statistics Add-Ins in MS Excel and GraphPad PRISM. Number of replicates was 8-10 (Figure 2A), 9-12 (Figure 2B), 8-12 (Figure 2D), 12-17 (Figure 3), 51-65 (Figure 4A), 12-23 (Figure 4B), 11 (Figure 5A), 9 (Figure 5B), 7-14 (Figure 6B), 12-14 (Figure 6C), 7 (Figure 6D).

Molecular Biology

The *UAS-FLII^{12}Pglu-700μδ KDEL* was generated from the expression plasmid pEF/myc/ER *FLII^{12}Pglu-700μδ6* (Addgene). The glucose sensor coding sequence was excised using PstI and XbaI. This fragment and a double stranded fragment encoding an ER targeting module (5'-GAATTCAGATCTGCCACC**ATG**GGATGGAGCTGTATCATCCTCTTCTTGGTAGCAACAGCTACAGGCG CGCACTCCCAGGTCCAACTGCAG-3'), cut with EcoRI and PstI, were cloned into the *pUAST* vector, which was cut with EcoRI and XbaI. This construct was injected into *w^{1118}* embryos (Bestgene, Inc).

Generation of *FMRFa* null mutations: *FMRFa* mutation was generated using CRISPR/Cas9 mutagenesis. The guide RNA (gRNA) was designed to anneal to nucleotides 175 to 194 downstream of the translation start codon (nucleotide 1) of the *FMRFa* gene. Complementary oligos were annealed and cloned into the pCFD3-dU6:3gRNA vector (Addgene #49410). The vector was introduced into *vermillion* (*v*) strain and crossed with *Act5C-Cas9* flies (Bloomington #54590). Approximately 10 progenies were collected and established as independent lines. Each fly within the established lines were sequenced. The deletion in *ΔFMRFa* removes almost 900 nucleotides (175 to 1063) encoding all 14 *FMRFa* peptides.

Immunostaining

Fly brains and thoracic ganglions were dissected in 1xPBS and then fixed in 4% paraformaldehyde with 0.2% Triton X-100 for 30 min at room temperature. Fixed brains were washed three times with PBS with 0.2% Triton X-100. The samples were incubated in blocking buffer (5% heat-inactivated goat serum) with 0.2% Triton X-100 for 30 min at room temperature. Then, samples were incubated with 1/1000 diluted primary antibodies for 1-2 days at 4 ˚C. Samples were washed three times with PBS with 0.2% Triton X-100 and

incubated with 1/1000 diluted secondary antibodies for 1-2 days at 4 ˚C. Samples were washed three times with PBS with 0.2% Triton X-100 and mounting solution (Vectashield) was added. Primary antibodies used in this study include chicken anti-GFP (Thermo fisher Scientific), rabbit anti-mCherry (BioVision), rabbit anti-NPF (RayBiotech), mouse anti-Orcokinin-A (gift from Dr. Mizoguchi), rabbit anti-IPNa (gift from Dr. Thor), rabbit anti-Pdf (gift from Dr. Hardin), rabbit anti-FMRFa (RayBiotech). Secondary antibodies were anti-chicken Alexa488 (Thermo fisher Scientific), anti-rabbit Alexa555 (Thermo fisher Scientific) and anti-mouse Cy3 (The Jackson laboratory).

In vivo Glucose imaging

Glucose imaging of FMRF neuron in the thoracic ganglion was conducted analogously as reported for NPF brain neurons, with the following modifications: the thoracic ganglion was extracted from the thorax while liquid silicone was applied over the entire preparation to prevent desiccation and preserve intracellular homeostatic conditions. Imaging was performed with a Nikon eclipse Ti inverted microscope with 20x water objective, excitation and emission filter wheels, and a dichroic filter (Nikon; 89002). The light source was a Lumen 200 lamp (Prior Scientific Inc). Data acquisition was performed with NIS-Elements software (Nikon). Three images were obtained to calculate FRET, 420-445 nm excitation and 470 nm emission with 400 ms exposure (Dd), 420-445 nm excitation and 530 nm emission with 100 ms exposure (Da), 500-517 nm excitation and 530 emission with 100 ms exposure (Aa). For data analysis, backgrounds were subtracted from all images. Dd and Aa spillovers (measured as 0.290 and 0.095, respectively) were also subtracted from Da. FRET efficiency was calculated using the formula Da-0.29xDd-0.095xAa)/Dd.

Golgi size measurement

The Golgi apparatus was visualized using *UAS-ManII-eGFP* expressed by respective GAL4 drivers. Golgi and neuropeptide staining was performed as described in Immunostaining except for using 4% paraformaldehyde with 0.01% Triton X-100 for fixation. All images were taken using a Nikon A1 confocal microscope with 60 x oil lens. Golgi and neuropeptide images were stacked (0.5 µm section intervals) and analyzed using ImageJ. Background was subtracted by thresholding using MaxEntropy for Golgi, Huang or Mean for neuropeptides,

and remained pixel numbers were counted. Golgi area was determined as the fraction of the area positive for NP, which served as a proxy for the cytosol.

Metabolic Analyses

Glucose/trehalose measurements: For glucose and trehalose measurements, a single male fly was homogenized in 100 μl of water. After heat-inactivation at 95 ˚C for 5 min, non-soluble debris was removed by centrifugation for 10 minutes at 14000 rpm and soluble fraction was transferred to a new Eppendorf tube. 5 μl of the soluble fraction was used for determination of glucose and trehalose content, respectively. Glucose was determined by adding 100 μl of Infinity™ Glucose Hexokinase Reagent (Thermo Scientific) to 5 μl of the soluble fraction for 10 minutes at 37 ˚C. Absorbance was measured at 340 nm using a Genesys 20 spectrophotometer (Thermo Scientific) and quantified against a standard glucose curve. For trehalose measurement, 5 μl of porcine kidney trehalase (2.3 units/mg; T8778-1UN, Sigma) was added to 5 μl of the soluble fraction for 30 minutes at 37 ˚C, followed the addition of 100 μl of the Infinity™ Glucose Hexokinase Reagent. Absorbance was measured as for glucose, and final trehalose amount was determined by deducting glucose content of the same fly sample. Fed flies were taken straight from standard food, while starved flies are flies kept on 1% agarose for 24 hours prior measurement.

Glycogen measurement: Adult males were anesthetized by CO_2. The abdomen and head were removed, the thorax separated into the dorsal (flight muscle) and the ventral halves (jump muscle). Jump muscles from three flies were placed into an Eppendorf tube containing 50 μl of 0.2 % NP-40 and stored at - 80 ˚C, until further processing. For measurements, samples were thawed, homogenized using a plastic pestle, and non-soluble debris was separated by centrifugation at 4 ˚C for 20 minutes at 14000 rpm. 5 μl of the supernatant was incubated with 5 μg of amyloglucosidase (Sigma- Aldrich A1602) with 50 mM Na acetate for 30 minutes at 37 ˚C. The aliquot was mixed with 100 μl of Infinity™ Glucose Hexokinase Reagent and incubated for 10 minutes at 37 ˚C, before absorbance was measured at 340 nm. Glycogen amount was obtained by subtraction of free glucose which was determined by measuring 340 nm absorbance of 5 μl of the same sample in the absence of amyloglucosidase. Samples were normalized to total amount of protein, which was determined using 20 μl of supernatant, to which with 20 μl water was added. 2.5 μl of this was mixed with 100 μl of

Bradford reagent (Bio-Rad #5000205) and absorbance was taken at 595 nm to calculate protein concentration against a standard curve.

Hemolymph neuropeptide measurements

For hemolymph collection, posterior end of the abdomen of ten flies was punctured and transferred in an iced Eppendorf tube containing 60 µl of PBS with 0.2 % Tween20. Flies were submerged in the buffer by spinning samples for 1 minute at 3000 × g in a microcentrifuge, followed by vortexing at speed 10 (Fisher Scientific Vortex mixer) for 10 minutes. Debris was removed by centrifugation for 1 minute at 3000 × g, and the supernatant (hemolymph) was transferred to a new tube.

ELISA was performed in triplicates using the ANP ELISA kit (Abcam #ab108797). Briefly, 50 µl of samples and standard titration in the range from 0.008 ng/mL to 2 ng/mL were added to each precoated well. The plate was fully sealed and incubated for 2-3 hours, followed by 4-5 washes with 200 µl of wash buffer. 50 µl of Biotinylated ANP antibody was added and incubated for 2 hours at room temperature. The wells were washed three times and 50 µl of Streptavidin-Peroxidase conjugate was added. After 30 minutes, the wells were washed once. 50 µl of chromogen substrate was added and incubated for 20 minutes or until the desired blue color was achieved, after which the reaction was terminated by adding 50 µl of the stop solution. Absorbance was measured immediately at 450nm using a microplate reader (BioTek Instruments Inc).

Measurement of Ilp2HF in the hemolymph was performed using the *Ilp2*^{1} *gd2HF* flies as described previously (Park et al 2014). Plates (Nunc Immuno clear modules; Thermo Fisher Scientific 468667) were coated with anti-Flag antibody (Sigma-Aldrich F1804) diluted in 0.2 M sodium carbonate/bicarbonate buffer (pH 9.4) to a final concentration of 2.5µg/mL. Plates were incubated overnight at 4 ˚C, washed twice using PBS containing 0.2% Tween 20. The wells were coated with 350µL PBS containing 2% BSA overnight, washed three times with PBS containing 0.2% Tween 20. The hemolymph was extracted in the same way as Anf-GFP, described above. 50µL of hemolymph containing solution or FLAG(GS)HA peptide standard (DYKDDDDKGGGGSYPYDVPDYAamide, life-Tein LLC) was mixed with 50µl of PBS containing 1% Tween20 and 5ng/mL anti-HA-Peroxidase 3F10 antibody (Roche #12013819001) and transferred to the wells. Plates were sealed and incubated overnight at 4 ˚C. Samples were removed and wells were washed six times with PBS with 0.2% Tween20. 100µL of 1-Step Ultra

TMB ELISA substrate (Thermo Fisher Scientific #34028) was added to each well, and plates were gently agitated for 30 minutes at room temperature. The reaction was stopped by adding 100µL of 2M sulfuric acid, and absorbance was measured immediately at 450nm.

REFERENCES (50)

Baines, R.A., Uhler, J.P., Thompson, A., Sweeney, S.T., Bate, M., 2001. Altered electrical properties in Drosophila neurons developing without synaptic transmission. J Neurosci 21, 1523–1531. https://doi.org/10.1523/JNEUROSCI.21-05-01523.2001

Banka, S., Chervinsky, E., Newman, W.G., Crow, Y.J., Yeganeh, S., Yacobovich, J., Donnai, D., Shalev, S., 2011. Further delineation of the phenotype of severe congenital neutropenia type 4 due to mutations in G6PC3. Eur J Hum Genet 19, 18–22. https://doi.org/10.1038/ejhg.2010.136

Bosma, K.J., Rahim, M., Singh, K., Goleva, S.B., Wall, M.L., Xia, J., Syring, K.E., Oeser, J.K., Poffenberger, G., McGuinness, O.P., Means, A.L., Powers, A.C., Li, W.-H., Davis, L.K., Young, J.D., O'Brien, R.M., 2020. Pancreatic islet beta cell-specific deletion of G6pc2 reduces fasting blood glucose. J Mol Endocrinol 64, 235–248. https://doi.org/10.1530/JME-20-0031

Bryantsev, A.L., Baker, P.W., Lovato, T.L., Jaramillo, M.S., Cripps, R.M., 2012. Differential requirements for Myocyte Enhancer Factor-2 during adult myogenesis in Drosophila. Dev Biol 361, 191–207. https://doi.org/10.1016/j.ydbio.2011.09.031

Cheung, Y.Y., Kim, S.Y., Yiu, W.H., Pan, C.-J., Jun, H.-S., Ruef, R.A., Lee, E.J., Westphal, H., Mansfield, B.C., Chou, J.Y., 2007. Impaired neutrophil activity and increased susceptibility to bacterial infection in mice lacking glucose-6-phosphatase-beta. J Clin Invest 117, 784–793. https://doi.org/10.1172/JCI30443

Chini, B., 2019. Expanding neuropeptide signalling by multiplying receptor functional states and sub-cellular locations. Cell Tissue Res 375, 49–56. https://doi.org/10.1007/s00441-018-2923-x

Chung, B.Y., Ro, J., Hutter, S.A., Miller, K.M., Guduguntla, L.S., Kondo, S., Pletcher, S.D., 2017. Drosophila Neuropeptide F Signaling Independently Regulates Feeding and Sleep-Wake Behavior. Cell Rep 19, 2441–2450. https://doi.org/10.1016/j.celrep.2017.05.085

Demontis, F., Piccirillo, R., Goldberg, A.L., Perrimon, N., 2013. The influence of skeletal muscle on systemic aging and lifespan. Aging Cell 12, 943–949. https://doi.org/10.1111/acel.12126

Deng, B., Li, Q., Liu, X., Cao, Y., Li, B., Qian, Y., Xu, R., Mao, R., Zhou, E., Zhang, W., Huang, J., Rao, Y., 2019. Chemoconnectomics: Mapping Chemical Transmission in Drosophila. Neuron 101, 876-893.e4. https://doi.org/10.1016/j.neuron.2019.01.045

Gauthier, S.A., Hewes, R.S., 2006. Transcriptional regulation of neuropeptide and peptide hormone expression by the Drosophila dimmed and cryptocephal genes. J Exp Biol 209, 1803–1815. https://doi.org/10.1242/jeb.02202

Gomarasca, M., Banfi, G., Lombardi, G., 2020. Myokines: The endocrine coupling of skeletal muscle and bone. Adv Clin Chem 94, 155–218. https://doi.org/10.1016/bs.acc.2019.07.010

Hardt, B., Völker, C., Mundt, S., Salska-Navarro, M., Hauptmann, M., Bause, E., 2005. Human endo-alpha1,2-mannosidase is a Golgi-resident type II membrane protein. Biochimie 87, 169–179. https://doi.org/10.1016/j.biochi.2004.11.004

Hayee, B., Antonopoulos, A., Murphy, E.J., Rahman, F.Z., Sewell, G., Smith, B.N., McCartney, S., Furman, M., Hall, G., Bloom, S.L., Haslam, S.M., Morris, H.R., Boztug, K., Klein, C., Winchester, B., Pick, E., Linch, D.C., Gale, R.E., Smith, A.M., Dell, A., Segal, A.W., 2011. G6PC3 mutations are associated with a major defect of glycosylation: a novel mechanism for neutrophil dysfunction. Glycobiology 21, 914–924. https://doi.org/10.1093/glycob/cwr023

Herzog, H., Darby, K., Ball, H., Hort, Y., Beck-Sickinger, A., Shine, J., 1997. Overlapping gene structure of the human neuropeptide Y receptor subtypes Y1 and Y5 suggests coordinate transcriptional regulation. Genomics 41, 315–319. https://doi.org/10.1006/geno.1997.4684

Hewes, R.S., Park, D., Gauthier, S.A., Schaefer, A.M., Taghert, P.H., 2003. The bHLH protein Dimmed controls neuroendocrine cell differentiation in Drosophila. Development 130, 1771–1781. https://doi.org/10.1242/dev.00404

Higuchi, H., Hasegawa, A., Yamaguchi, T., 2005. Transcriptional regulation of neuronal genes and its effect on neural functions: transcriptional regulation of neuropeptide Y gene by leptin and its effect on feeding. J Pharmacol Sci 98, 225–231. https://doi.org/10.1254/jphs.fmj05001x6

Hoyer, D., Bartfai, T., 2012. Neuropeptides and neuropeptide receptors: drug targets, and peptide and non-peptide ligands: a tribute to Prof. Dieter Seebach. Chem Biodivers 9, 2367–2387. https://doi.org/10.1002/cbdv.201200288

Husain, Q.M., Ewer, J., 2004. Use of targetable gfp-tagged neuropeptide for visualizing neuropeptide release following execution of a behavior. J Neurobiol 59, 181–191. https://doi.org/10.1002/neu.10309

Jun, H.S., Lee, Y.M., Cheung, Y.Y., McDermott, D.H., Murphy, P.M., De Ravin, S.S., Mansfield, B.C., Chou, J.Y., 2010. Lack of glucose recycling between endoplasmic reticulum and cytoplasm underlies cellular dysfunction in glucose-6-phosphatase-beta-deficient neutrophils in a congenital neutropenia syndrome. Blood 116, 2783–2792. https://doi.org/10.1182/blood-2009-12-258491

Kneen, M., Farinas, J., Li, Y., Verkman, A.S., 1998. Green fluorescent protein as a noninvasive intracellular pH indicator. Biophys J 74, 1591–1599. https://doi.org/10.1016/S0006-3495(98)77870-1

Kondylis, V., Rabouille, C., 2009. The Golgi apparatus: lessons from Drosophila. FEBS Lett 583, 3827–3838. https://doi.org/10.1016/j.febslet.2009.09.048

Landayan, D., Wang, B.P., Zhou, J., Wolf, F.W., 2021. Thirst interneurons that promote water seeking and limit feeding behavior in Drosophila. Elife 10. https://doi.org/10.7554/eLife.66286

Lear, B.C., Zhang, L., Allada, R., 2009. The neuropeptide PDF acts directly on evening pacemaker neurons to regulate multiple features of circadian behavior. PLoS Biol 7, e1000154. https://doi.org/10.1371/journal.pbio.1000154

Lee, K.-S., You, K.-H., Choo, J.-K., Han, Y.-M., Yu, K., 2004. Drosophila short neuropeptide F regulates food intake and body size. J Biol Chem 279, 50781–50789. https://doi.org/10.1074/jbc.M407842200

Liu, W., Ganguly, A., Huang, J., Wang, Y., Ni, J.D., Gurav, A.S., Aguilar, M.A., Montell, C., 2019. Neuropeptide F regulates courtship in Drosophila through a male-specific neuronal circuit. Elife 8. https://doi.org/10.7554/eLife.49574

Lu, T.-C., Brbić, M., Park, Y.-J., Jackson, T., Chen, J., Kolluru, S.S., Qi, Y., Katheder, N.S., Cai, X.T., Lee, S., Chen, Y.-C., Auld, N., Liang, C.-Y., Ding, S.H., Welsch, D., D'Souza, S., Pisco, A.O., Jones, R.C., Leskovec, J., Lai, E.C., Bellen, H.J., Luo, L., Jasper, H., Quake, S.R., Li, H., 2023. Aging Fly Cell Atlas identifies exhaustive aging features at cellular resolution. Science 380, eadg0934. https://doi.org/10.1126/science.adg0934

Lundquist, T., Nässel, D.R., 1990. Substance P-, FMRFamide-, and gastrin/cholecystokinin-like immunoreactive neurons in the thoraco-abdominal ganglia of the flies Drosophila and Calliphora. J Comp Neurol 294, 161–178. https://doi.org/10.1002/cne.902940202

Matsuda, H., Yamada, T., Yoshida, M., Nishimura, T., 2015. Flies without trehalose. J Biol Chem 290, 1244–1255. https://doi.org/10.1074/jbc.M114.619411

Miyamoto, T., Amrein, H., 2019. Neuronal Gluconeogenesis Regulates Systemic Glucose Homeostasis in Drosophila melanogaster. Curr Biol 29, 1263-1272.e5. https://doi.org/10.1016/j.cub.2019.02.053

Miyamoto, T., Amrein, H., 2017. Gluconeogenesis: An ancient biochemical pathway with a new twist. Fly (Austin) 11, 218–223. https://doi.org/10.1080/19336934.2017.1283081

Nässel, D.R., Zandawala, M., 2019. Recent advances in neuropeptide signaling in Drosophila, from genes to physiology and behavior. Prog Neurobiol 179, 101607. https://doi.org/10.1016/j.pneurobio.2019.02.003

Paradis, S., Sweeney, S.T., Davis, G.W., 2001. Homeostatic control of presynaptic release is triggered by postsynaptic membrane depolarization. Neuron 30, 737–749. https://doi.org/10.1016/s0896-6273(01)00326-9

Parisky, K.M., Agosto, J., Pulver, S.R., Shang, Y., Kuklin, E., Hodge, J.J.L., Kang, K., Liu, X., Garrity, P.A., Rosbash, M., Griffith, L.C., 2008. PDF cells are a GABA-responsive wake-promoting component of the Drosophila sleep circuit. Neuron 60, 672–682. https://doi.org/10.1016/j.neuron.2008.10.042

Park, S., Alfa, R.W., Topper, S.M., Kim, G.E.S., Kockel, L., Kim, S.K., 2014. A genetic strategy to measure circulating Drosophila insulin reveals genes regulating insulin production and secretion. PLoS Genet 10, e1004555. https://doi.org/10.1371/journal.pgen.1004555

Rai, M., Demontis, F., 2016. Systemic Nutrient and Stress Signaling via Myokines and Myometabolites. Annu Rev Physiol 78, 85–107. https://doi.org/10.1146/annurev-physiol-021115-105305

Ravi, P., Trivedi, D., Hasan, G., 2018. FMRFa receptor stimulated Ca2+ signals alter the activity of flight modulating central dopaminergic neurons in Drosophila melanogaster. PLoS Genet 14, e1007459. https://doi.org/10.1371/journal.pgen.1007459

Renn, S.C., Park, J.H., Rosbash, M., Hall, J.C., Taghert, P.H., 1999. A pdf neuropeptide gene mutation and ablation of PDF neurons each cause severe abnormalities of behavioral circadian rhythms in Drosophila. Cell 99, 791–802. https://doi.org/10.1016/s0092-8674(00)81676-1

Schneider, L.E., Roberts, M.S., Taghert, P.H., 1993a. Cell type-specific transcriptional regulation of the Drosophila FMRFamide neuropeptide gene. Neuron 10, 279–291. https://doi.org/10.1016/0896-6273(93)90318-l

Schneider, L.E., Sun, E.T., Garland, D.J., Taghert, P.H., 1993b. An immunocytochemical study of the FMRFamide neuropeptide gene products in Drosophila. J Comp Neurol 337, 446–460. https://doi.org/10.1002/cne.903370308

Shao, L., Saver, M., Chung, P., Ren, Q., Lee, T., Kent, C.F., Heberlein, U., 2017. Dissection of the Drosophila neuropeptide F circuit using a high-throughput two-choice assay. Proc Natl Acad Sci U S A 114, E8091–E8099. https://doi.org/10.1073/pnas.1710552114

Silva, V., Palacios-Muñoz, A., Volonté, M., Frenkel, L., Ewer, J., Ons, S., 2021. Orcokinin neuropeptides regulate reproduction in the fruit fly, Drosophila melanogaster. Insect Biochem Mol Biol 139, 103676. https://doi.org/10.1016/j.ibmb.2021.103676

Thompson, S.N., 2003. Trehalose – The Insect 'Blood' Sugar. Advances in Insect Physiology 31, 205–285. https://doi.org/10.1016/S0065-2806(03)31004-5

van den Pol, A.N., 2012. Neuropeptide transmission in brain circuits. Neuron 76, 98–115. https://doi.org/10.1016/j.neuron.2012.09.014

van Schaftingen, E., Gerin, I., 2002. The glucose-6-phosphatase system. Biochem J 362, 513–532. https://doi.org/10.1042/0264-6021:3620513

Veiga-da-Cunha, M., Chevalier, N., Stephenne, X., Defour, J.-P., Paczia, N., Ferster, A., Achouri, Y., Dewulf, J.P., Linster, C.L., Bommer, G.T., Van Schaftingen, E., 2019. Failure to eliminate a phosphorylated glucose analog leads to neutropenia in patients with G6PT and G6PC3 deficiency. Proc Natl Acad Sci U S A 116, 1241–1250. https://doi.org/10.1073/pnas.1816143116

Verleyen, P., Baggerman, G., Wiehart, U., Schoeters, E., Van Lommel, A., De Loof, A., Schoofs, L., 2004. Expression of a novel neuropeptide, NVGTLARDFQLPIPNamide, in the larval and adult brain of Drosophila melanogaster. J Neurochem 88, 311–319. https://doi.org/10.1046/j.1471-4159.2003.02161.x

Volkenhoff, A., Weiler, A., Letzel, M., Stehling, M., Klämbt, C., Schirmeier, S., 2015. Glial Glycolysis Is Essential for Neuronal Survival in Drosophila. Cell Metab 22, 437–447. https://doi.org/10.1016/j.cmet.2015.07.006

Wu, Q., Wen, T., Lee, G., Park, J.H., Cai, H.N., Shen, P., 2003. Developmental control of foraging and social behavior by the Drosophila neuropeptide Y-like system. Neuron 39, 147–161. https://doi.org/10.1016/s0896-6273(03)00396-9

Zhao, X., Karpac, J., 2017. Muscle Directs Diurnal Energy Homeostasis through a Myokine-Dependent Hormone Module in Drosophila. Curr Biol 27, 1941-1955.e6. https://doi.org/10.1016/j.cub.2017.06.004

Zhao, X., Li, X., Shi, X., Karpac, J., 2020. Diet-MEF2 interactions shape lipid droplet diversification in muscle to influence Drosophila lifespan. Aging Cell 19, e13172. https://doi.org/10.1111/acel.13172

Zhou, W., Chang, J., Wang, X., Savelieff, M.G., Zhao, Y., Ke, S., Ye, B., 2014. GM130 is required for compartmental organization of dendritic golgi outposts. Curr Biol 24, 1227–1233. https://doi.org/10.1016/j.cub.2014.04.008

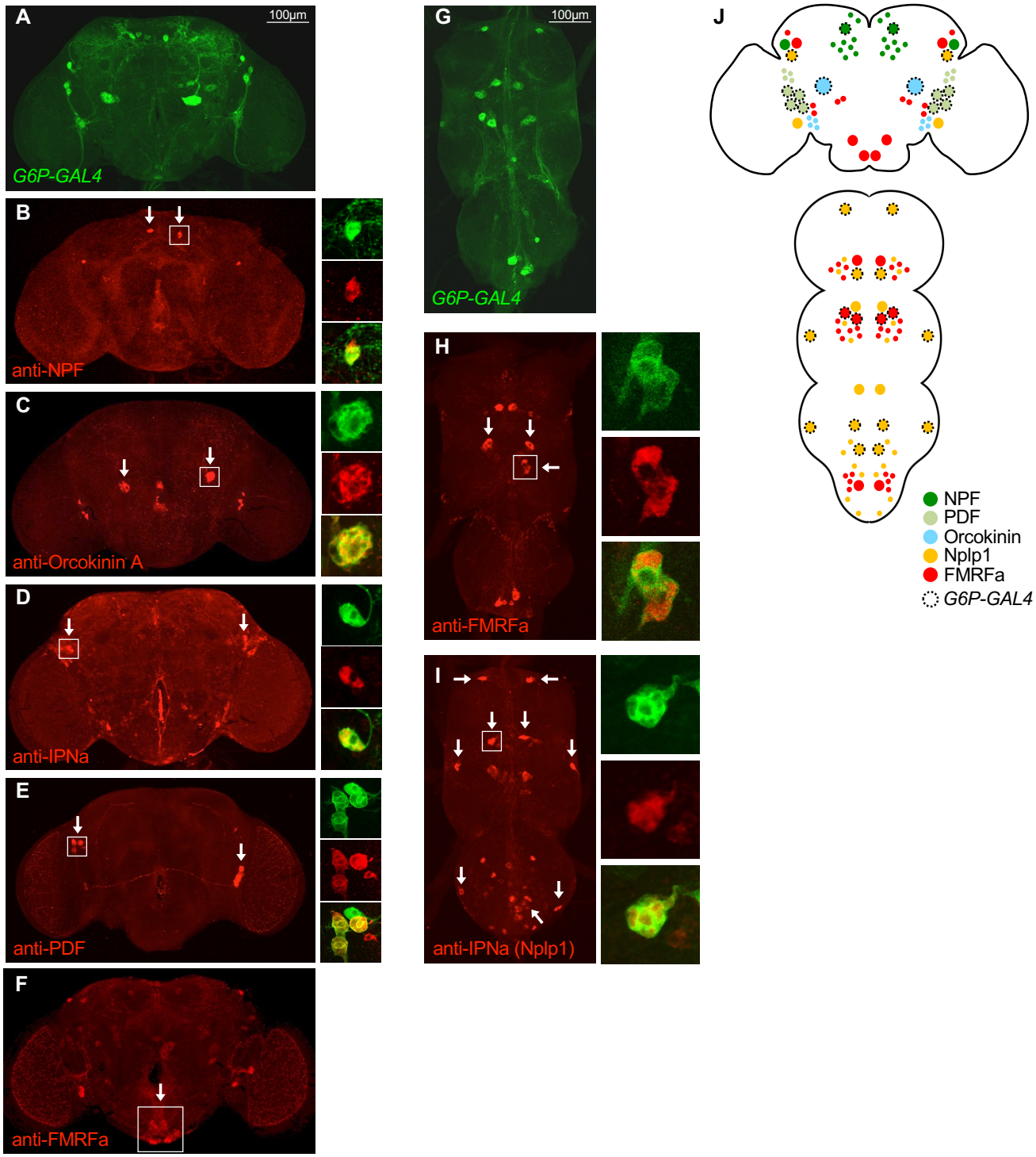
A
100µm
G6P-GAL4
B
anti-NPF
C
anti-Orcokinin A
D
anti-IPNa
E
anti-PDF
F
anti-FMRFa
G
100µm
G6P-GAL4
H
anti-FMRFa
I
anti-IPNa (Nplp1)
J
NPF
PDF
Orcokinin
Nplp1
FMRFa
G6P-GAL4

Figure 1

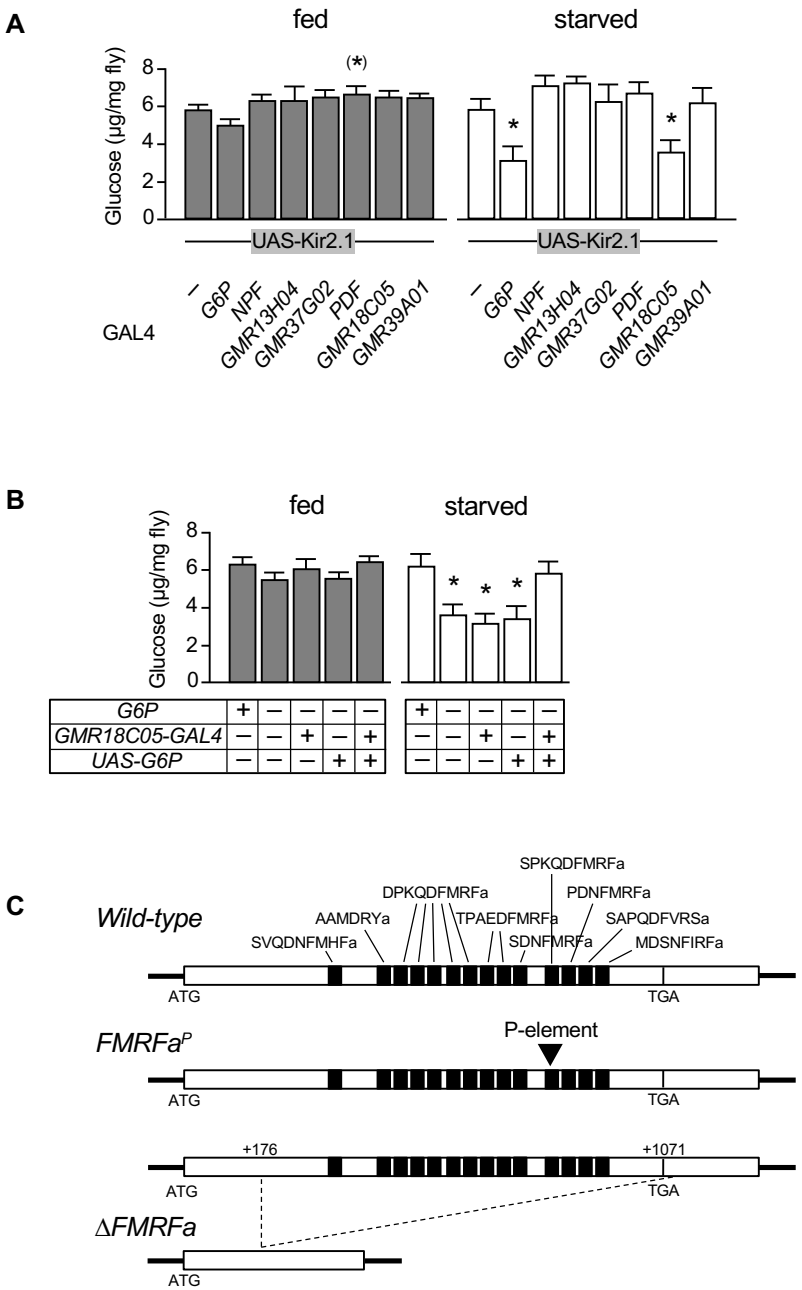
A
fed
starved
Glucose (µg/mg fly)
8
6
4
2
0
(*)
*
*
UAS-Kir2.1
UAS-Kir2.1
GAL4
/
G6P
NPF
GMR13H04
GMR37G02
PDF
GMR18C05
GMR39A01
B
fed
starved
Glucose (µg/mg fly)
G6P
GMR18C05-GAL4
UAS-G6P
C
Wild-type
SPKQDFMRFa
DPKQDFMRFa
PDNFMRFa
AAMDRYa
TPAEDFMRFa
SAPQDFVRSa
SVQDNFMHFa
SDNFMRFa
MDSNFIRFa
ATG
TGA
FMRFa^P
P-element
+176
+1071
ΔFMRFa
D
fed
starved
Glucose (µg/mg fly)
**
**
*
**
Wild
G6P^MIC
FMRFa^P
ΔFMRFa

Figure 2

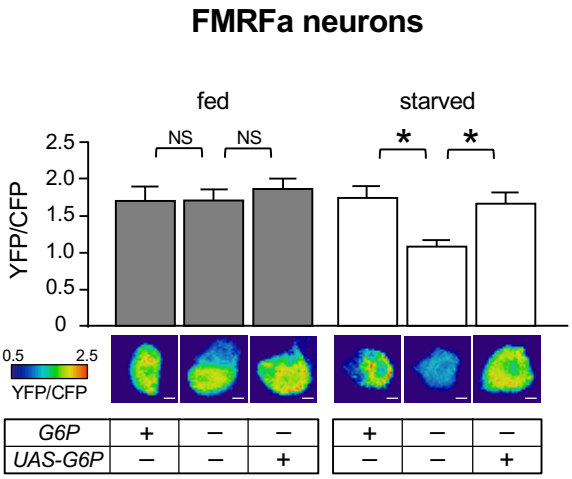
FMRFa neurons
fed
starved
NS
NS
*
*
YFP/CFP
2.5
2.0
1.5
1.0
0.5
0
0.5
2.5
YFP/CFP
G6P
UAS-G6P

Figure 3

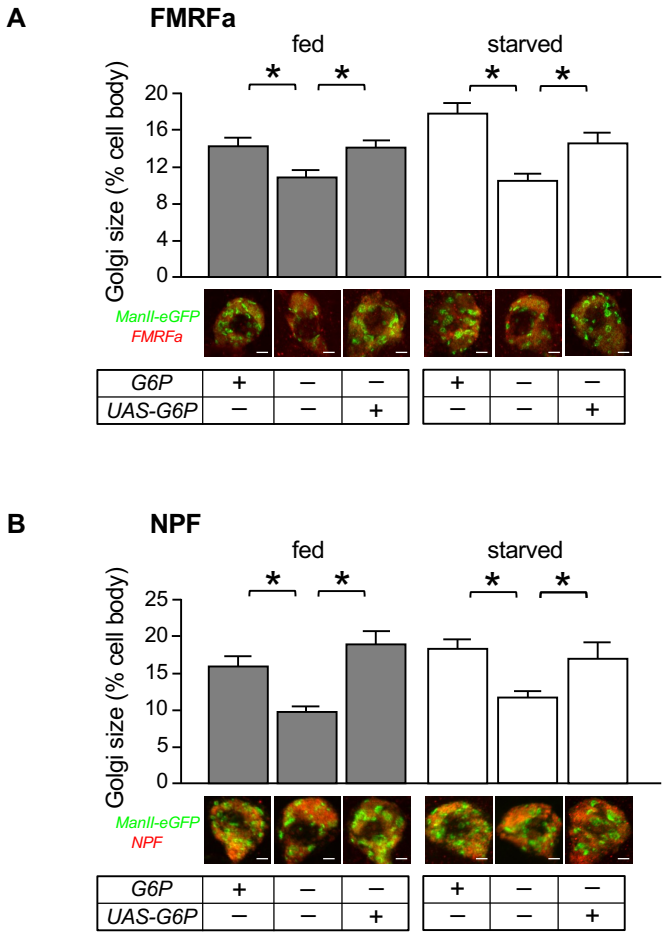
A
FMRFa
fed
starved
Golgi size (% cell body)
20
16
12
8
4
0
ManII-eGFP
FMRFa
G6P
UAS-G6P
B
NPF
fed
starved
Golgi size (% cell body)
25
20
15
10
5
0
ManII-eGFP
NPF
G6P
UAS-G6P

Figure 4

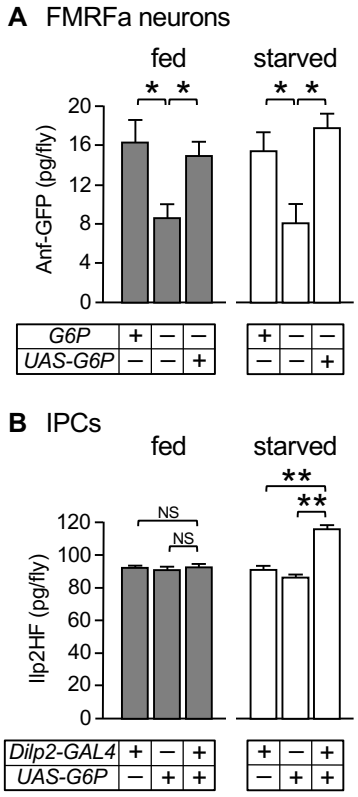
A FMRFa neurons
fed
starved
Anf-GFP (pg/fly)
20
16
12
8
4
0
*
*
*
*
G6P
UAS-G6P
B IPCs
fed
starved
Ilp2HF (pg/fly)
120
100
80
60
40
20
0
NS
NS
**
**
Dilp2-GAL4
UAS-G6P

Figure 5

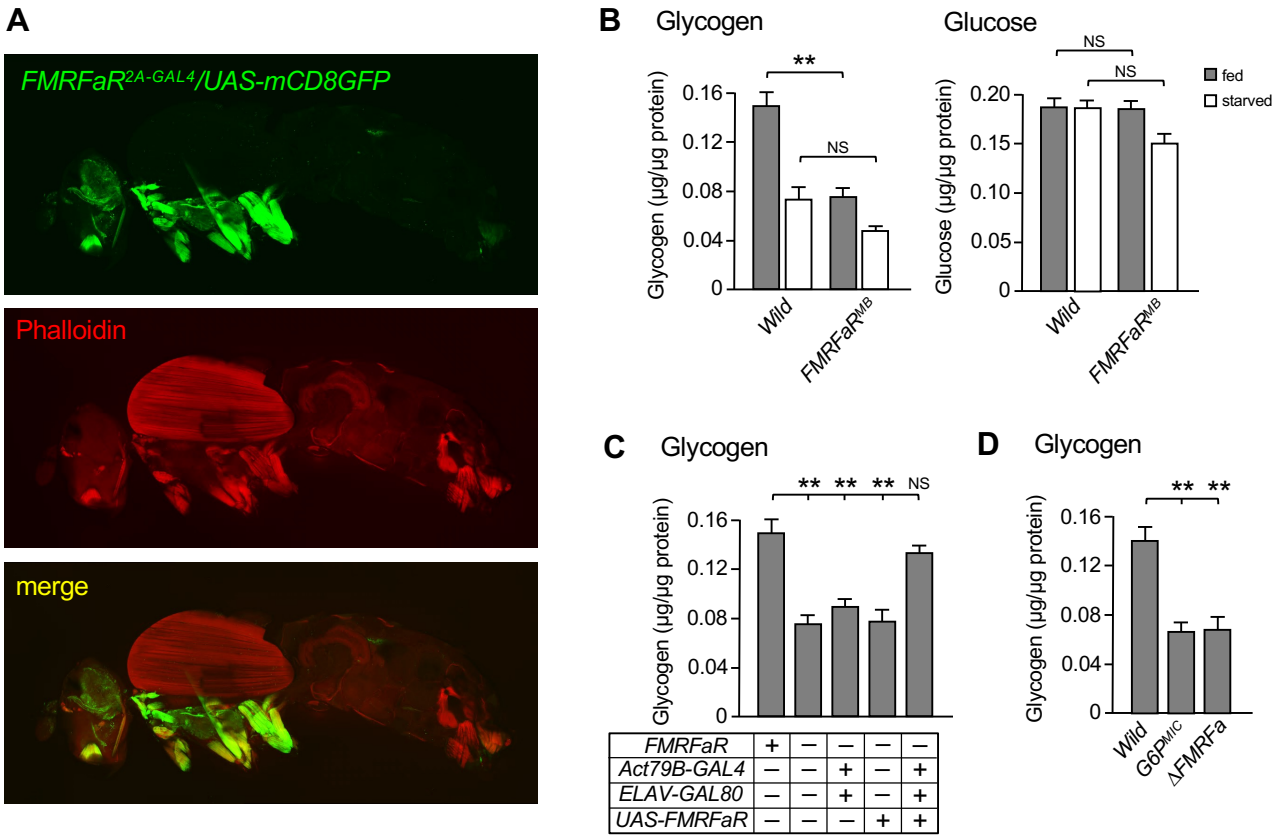
A
FMRFaR2A-GAL4/UAS-mCD8GFP
Phalloidin
merge
B
Glycogen
Glucose
Glycogen (µg/µg protein)
Glucose (µg/µg protein)
**
NS
fed
starved
Wild
FMRFaRMB
C
Glycogen
D
Glycogen
G6PMIC
ΔFMRFa
FMRFaR
Act79B-GAL4
ELAV-GAL80
UAS-FMRFaR

Figure 6